Journal of Structural Geology, Vol. 7, No. 2, pp. 251 to 266, 1985
Printed in Great Britain

0191-8141/85 $03.00 + 0.00

Experimental 'syntectonic' hydration of basalt

E. H. RUTTER, C. J. PEACH, S. H. WHITE and D. JOHNSTON

Geology Department, Imperial College, London, S.W.7, U.K.

(*Received* 7 *October* 1983; *accepted in revised form* 23 *July* 1984)

Abstract—This paper outlines in general terms the role of metamorphic transformations during rock deformation. Long duration, triaxial stress relaxation tests at 600°C, 160 MPa confining pressure on wet crushed basalt, sheared in sawcuts made in intact basalt cylinders are reported. Mechanical data are interpreted in terms of a material which shows a small strain-rate sensitivity to large variations in applied stress, but which work hardens dramatically as a result of marked microstructural changes which occur during straining. Permanent distortions of *c*. 20% were produced in the samples.

Tests at 100 MPa pore-water pressure resulted in the formation of oriented overgrowths of amphibole, preferentially developed on less stressed interfaces between original grains and in pore spaces. Substantial redistribution of feldspar also occurred. At low pore pressures no amphibole formed and only feldspar was recrystallized. Much of the original porosity of the rock was eliminated in all cases.

The mechanical and microstructural data are interpreted in terms of flow by some combination of grain sliding and diffusional accommodation, with the reprecipitated, diffused material being the product of a chemical reaction involving all original solid phases plus water. From a consideration of the effects of the reaction on the chemical potential gradients driving diffusion, it is concluded that although the syntectonic hydration exerts a profound effect on the microstructural and mineralogical development of the rock during deformation, there is no substantial enhancement of the rate of strain.

Similar microstructural developments also occur in natural rocks deformed during retrogressive metamorphic events, and examples are described for comparison.

INTRODUCTION

FOR MORE than 40 years, experimental studies of rock deformation have, with certain exceptions, been carried out either on monomineralic rocks or on polymineralic rocks under conditions where chemical transformations do not occur. This is a logical approach, and has led to a basic understanding of the fundamental mechanisms of rock deformation and of accompanying processes. However, it is widely recognized that a great deal, perhaps most, of natural rock deformation is accompanied by, or followed by, chemical or structural transformations.

To some extent, textural features of deformed rocks can be used to infer time relations between periods of mineral growth and deformation (Spry 1969, Vernon 1976) but the general effect of metamorphic changes is to complicate or destroy microstructural indicators of deformation mechanism(s). It is rarely possible to point to direct microstructural indicators of dominant deformation mechanism in polymineralic metamorphic tectonites, and this is further complicated by the fact that different minerals often behave in different ways in the same rock.

This paper aims to address briefly some of the questions of the interrelationships between deformation and metamorphism. Experimental data on the synmetamorphic deformation of a basaltic rock are presented and the geological implications are discussed.

ROLE OF METAMORPHIC TRANSFORMATIONS DURING ROCK DEFORMATION

The general topic of the interaction between deformation and metamorphism includes both the role of metamorphism in deformation and the role of deformation in metamorphism. The latter involves the enhancement of the kinetics of metamorphic transformation and the modifying of equilibrium relations. Such effects can occur, for example, through the tectonic reduction of grain size and through the accumulation of elastic energy in the form of dislocation arrays. However, this topic lies outside the scope of the present paper (but see Brodie & Rutter in press). We will restrict our attention below to the role of metamorphic transformations during deformation.

It is widely held that the episodic structural and chemical transformations that rocks suffer during a metamorphic cycle coincide with corresponding periods of enhanced deformability (mechanical softening). There may be several contributory mechanisms to enhanced deformability, dependent on mineralogy and metamorphic conditions. Such 'pulses' of enhanced strain rate or stress relaxation (depending on how the rock mass is loaded) will be superimposed on a 'background' strain rate due to processes occurring in the absence of metamorphic changes (Fig. 1). The 'background' strain rate, though trending upwards with increasing temperature, will fluctuate according to the mechanical properties of the new solid phases resulting from each transformation. For example, the rock may become harder during prograde metamorphism, and softer following retrograde changes. Mechanical softening during phase transformations is known to materials scientists under the general heading of 'transformational plasticity', and various different mechanisms may be involved for different materials (Chaklader 1975, Poirier 1982). Various aspects of the modification of deformability by mineral transformations during natural rock deformation have

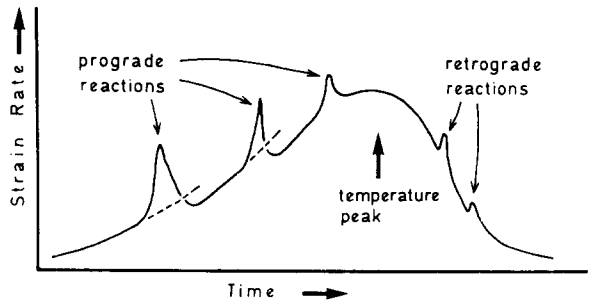

Fig. 1. Schematic illustration of variation in strain rate at constant stress during a metamorphic cycle. Peaks represent episodes of deformability enhancement associated with metamorphic transformations. Changes in 'background' strain rate following a reaction correspond to response to difference in mineralogy before and after the transformation event.

been considered by White & Knipe (1978), Poirier (1982), Gordon (1971), Sammis & Dein (1974), Fyfe (1976) and Brodie & Rutter (in press).

Metamorphic transformations can be conveniently subdivided into (a) those which occur without mass gain or loss (e.g. the basalt–eclogite transformation) and (b) those which involve mass gain or loss. For this paper we will be particularly concerned with the latter group, which is of particular importance in the deformation of crustal rocks. The mass gain or loss is dominantly of water and carbon dioxide, with the additional possibility of substantial quantities of silica, sodium, potassium, calcium and magnesium being moved about in the flux of pore fluid. There is usually a volume change of the solid phases, which under conditions of non-hydrostatic stress will manifest itself as a contribution to the distortional strain (Ramsay & Wood 1973, Beach 1982).

Quite separately from the strain due to volume change, the resistance of a rock to deformation during the metamorphic transformation may be modified in a number of ways. The relative importance of these processes will depend on the particular transformation, but it should be considered that some transformations may not be accompanied by mechanical softening at all. Some softening processes are listed below.

(1) Evolution of high pressure water or carbon dioxide during a dehydration or decarbonation reaction may lower effective confining pressure and facilitate cataclastic flow or faulting, provided the evolved fluid is not allowed to escape (undrained conditions). Such effects have been studied experimentally for serpentinite (Raleigh & Paterson 1965), gypsum (Heard & Ruby 1966) and for these and other hydrous minerals by Murrell & Ismail (1976).

(2) Reaction products may be transiently sufficiently fine grained so that flow by diffusion-accommodated grain boundary sliding is facilitated (e.g. Rubie 1983). Subsequent grain growth during slow creep between deformation episodes would be expected to eliminate textural evidence of this process.

(3) Volume changes in solid phases may induce local deviatoric stresses which assist the applied stress in overcoming the resistance to flow by intracrystalline plasticity. This phenomenon is most frequently invoked to explain transformation plasticity in metals and ceramics (Greenwood & Johnston 1965, Poirier 1982). At low effective pressures in rocks volume change may also induce cracking.

(4) The equilibrium point-defect chemistry of solid phases is modified through the progress of a chemical reaction or merely by changing the pressure of a volatile component (e.g. introducing water into a developing shear zone) (Hobbs 1981, Kirby 1984). This may facilitate any flow process which depends on solid-state diffusion, such as dislocation creep or Nabarro–Herring creep. The phenomenon of hydrolytic weakening of quartz may be included under this heading.

(5) When flow by water-assisted diffusive mass-transfer processes leads to precipitation of overgrowths which are of different mineralogical composition to the host grains (i.e. they are the products of a metamorphic reaction), the deformation mechanism can be termed "incongruent pressure solution" (Beach 1982). The chemical potential gradient driving the diffusive tansfer may be steepened through the volume-change terms in the free energy of the reaction, thus enhancing the strain rate through the diffusion kinetics (Beach 1982, Rutter 1983). The overgrowths are usually the products of a retrograde metamorphic reaction, produced through the partial destruction of a phase assemblage stable at higher temperature. Products of prograde transformations cannot normally be preserved in this way (Brodie & Rutter in press), except at low metamorphic grades, because the reactions tend to go to completion.

The behaviour of basalt under conditions favouring retrogressive metamorphism and hydration, as reported in this paper, is considered to fall into this latter category.

EXPERIMENTAL PROCEDURES

Deformation experiments

Apparatus. A fluid-confining-medium deformation apparatus able to operate leak-free at moderate pressures for periods up to two months, at temperatures up to 800°C, with independently controllable pore fluid pressure was required for this project. An externally heated pressure vessel, machined from Nimonic 110 alloy, using water as a confining pressure medium, was used (Fig. 2). The Nimonic loading piston is driven from the bottom of the pressure vessel via a ballscrew and gearbox. The semi-internal axial force gauge is carried in the moving piston. The sample assembly is loaded into the apparatus via the top closure, so the moving seal assembly is not normally dismantled between runs. The NiCr/NiAl specimen temperature thermocouple (Inconel sheathed) makes contact with the top of the cylindrical specimen via the hollow upper loading piston. The pore fluid is transmitted to the specimen via the same hole. The specimen is jacketed using 0.25 mm wall thickness annealed copper tubing. Water cooled, rubber 'O' ring pressure seals are used at each end of the pressure vessel.

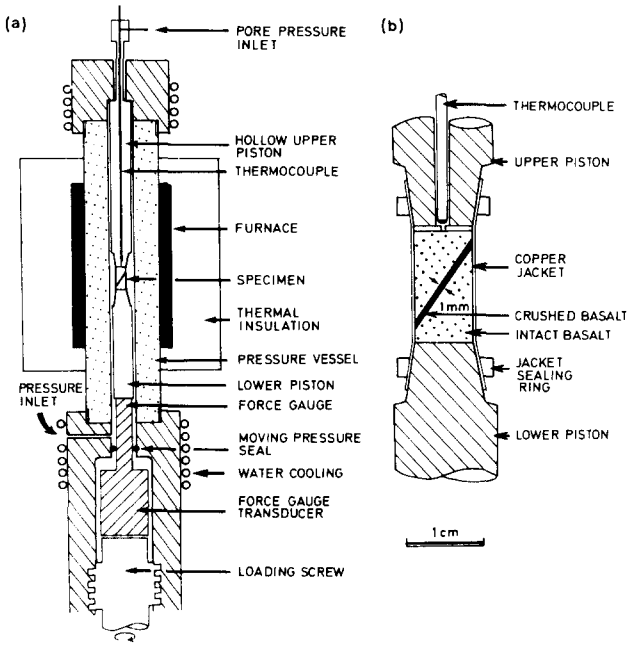

Fig. 2. (a) Schematic illustration of the main features of the deformation machine used for this study. (Not to relative scale, but assembly shown stands approximately 1.5 m high.) (b) Axial cross-section through the specimen configuration used.

Experiments. A very fresh basalt was sought, if possible free from hydrothermal alteration and uniformly fine grained. Large blocks were collected from a single column about 50 m above the base of a thick (*c.* 150 m) columnar mass, probably originating as a lava lake or thick ponded flow, on the north face of Preshal Mhor, near Talisker, Isle of Skye. This is a low alkali, high calcium olivine tholeiite of very uniform composition. Analyses by Esson *et al.* (1975) of two samples taken from the same cliff (their sample numbers 309 and 311) are reproduced in Table 3.

The rock is composed of plagioclase (55%), clinopyroxene (29%) and olivine (15%), with small amounts (3%) of opaque minerals. No optical evidence of glass or alteration products was seen, although slight localized grain boundary alteration was seen in some TEM foils. The rock possesses a good ophitic texture and the grain size is approximately 25 μm. Phenocrysts are rare. Average effective porosity was determined to be 1.4 ± 1% (range) by means of water saturation under vacuum.

Initially it was intended to use the stress relaxation technique in the way described by Rutter & Mainprice (1978) on cylinders of basalt pre-faulted at 200 MPa confining pressure at 20°C, so that a fine grained 'gouge' zone of moderate initial porosity would be produced, and in which chemical transformation would be expected to be facilitated during subsequent high temperature deformation in the presence of water. However, it was found that this rock was extremely strong, supporting a differential stress of 1.4 GPa at 200 MPa confining pressure. This frequency resulted in damage to the loading pistons and the failure was often so violent that the copper jacket was ruptured. Synthetic basalt 'gouge' was therefore prepared by grinding and sieving the rock to less than 90 μm, followed by further grinding to produce a powder of about 5–15 μm particle size. A stiff paste of this material, 1 mm thick, was then sheared in sawcuts made at 35° to the axis of intact basalt cylinders, 6.35 mm diameter × 18 mm long (Fig. 2).

In the stress relaxation testing method, the rock sample is loaded rapidly to some level of differential stress, whereupon the length of the specimen plus a portion of the machine is held constant. The stored elastic energy of the machine plus specimen then is slowly dissipated through the accumulation of permanent strain in the specimen, and the differential stress relaxes. Knowing the mechanical compliances of the system, the permanent strain rate at each point during the decay of stress can be calculated. The application of the method is discussed by Rutter *et al.* (1978).

In some experiments the pore water was permitted access to the gouge zone only by permeation through the upper half of the cut basalt cylinder. In others, a narrow hole was drilled through the upper specimen half, to be quite sure that the pore pressure was applied directly to the gouge zone. In the former case, pore filling neomineralization coupled with the intrinsic low permeability of fine-grained igneous rocks was expected to decouple the pore pressure in the gouge zone from the remainder of the pore pressure system, possibly leading to anomalous mechanical effects due to unknown effective confining pressure. The disadvantage of the latter configuration, however, is that substantial hydrothermal transport of specimen components along the pore pressure pipe might be expected. In practice however, there was no systematic difference in the mechanical behaviour of the two arrangements except for the case of specimen PMB4/14.

From a chemical standpoint, the effective rock/water ratio is strikingly different in the two experimental configurations. Oxygen activity will also differ in the sample pores because of differences in proximity to the copper- and nickel-rich parts of the specimen/piston/jacket assembly. The problems of performing deformation experiments under satisfactorily controlled chemical conditions remains to be addressed further. The use of a natural rock in an experimental system which is difficult to control chemically means that at this time only qualitative statements may be made about the chemical changes which accompanied deformation.

Experiments performed. Two series of experiments are reported here.

(a) Gouge filled sawcut samples were sheared rapidly (6×10^{-6} m s^{-1} axial shortening rate) in order to determine the frictional characteristics of the gouge at 20°C at various confining pressures, and at 600°C at 200 MPa confining pressure with various pore pressures. The experimental data are shown in Fig. 3. These experiments permitted the applicability of the effective stress principle to be evaluated at 20°C and 600°C together with an indication of the effects of wetting and of a large temperature change on the high strain rate strength of the gouge.

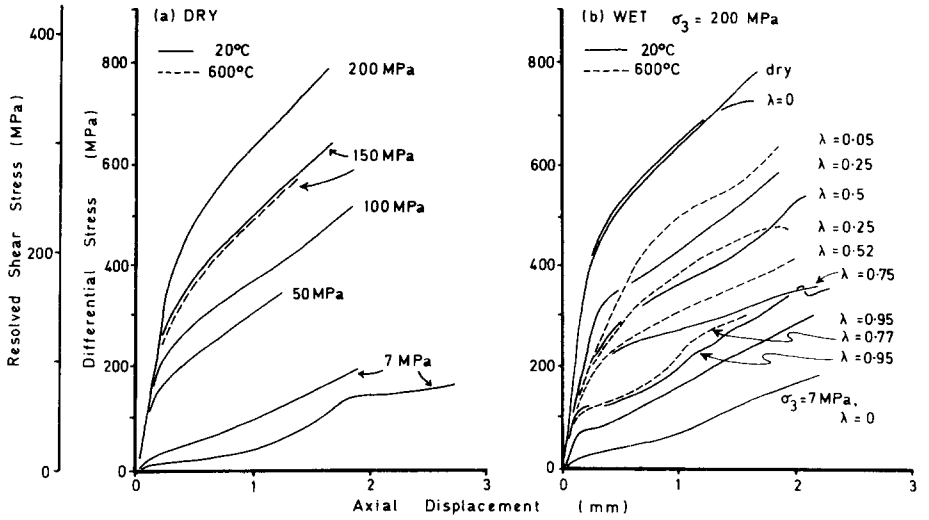

Fig. 3. Differential stress vs total axial displacement curves for samples deformed at 20 and 600°C, dry at confining pressures indicated (a), and wet at 200 MPa confining pressure at various pore pressures (b). λ = pore pressure/total confining pressure. A dry test at 200 MPa is also shown in (b) for comparison. A list of experimental details is given in Table 1. Axial piston displacement rate in all cases = 6×10^{-6} m s^{-1}. A scale of resolved shear stress along the sawcut is also shown.

(b) A series of stress-relaxation experiments of 2–40 days duration were performed on wet and dry samples at *c.* 170 MPa total confining pressure. Pore pressures of *c.* 20 MPa and 100 MPa were used. One test was run wet with the sawcut 90° to the cylinder axis to evaluate the effects of specimen compaction in the absence of shearing forces, and one test was run under hydrostatic conditions with pore pressure equal to confining pressure. All experiments were performed at 600°C so that most amphiboles would be stable. No attempt has yet been made to investigate the effects of temperature variations in long duration experiments.

A listing of experimental conditions for the reported test is given in Tables 1 and 2.

Microstructural studies

Extra thin optical sections were made from all successful high temperature experimental samples. All samples which were deformed wet for many days at 600°C were hard and completely lithified. Samples deformed dry at all conditions remained friable. From some samples ion-thinned specimens were prepared for scanning–transmission (TEMSCAN) electron microscopy. From these samples some 120 energy dispersive chemical analyses were obtained from pre-existing and newly grown phases (Figs. 9–11). Both broken and polished sample surfaces were also examined by scanning electron microscopy. Attempts were made to study the

Table 1. Constant displacement rate tests (6×10^{-6} m s^{-1} piston displacement rate)

Test	Wet/dry	Temp. °C	Conf. Press. MPa	Hollow spec.?	Pore Press. MPa
1A/3	dry	20	200	no	0
1A/15	dry	20	200	no	0
1A/16	dry	20	150	no	0
1A/2	dry	20	100	no	0
1A/4	dry	20	50	no	0
1A/5	dry	20	7	no	0
1A/19	dry	20	7	no	0
4/21	dry	600	150	no	0
1A/6	wet	20	7	no	0
1A/11	wet	20	200	no	0
1A/12	wet	20	200	no	50
1A/17	wet	20	200	no	50
1A/13	wet	20	200	no	100
1A/9	wet	20	200	no	100
1A/10	wet	20	200	no	150
1A/20	wet	20	200	no	190
1A/21	wet	20	200	yes	190
1A/26	wet	600	200	no	10
1A/27	wet	600	200	no	50
1A/25	wet	600	200	no	104
1A/23	wet	600	200	no	138
1A/23	wet	600	200	no	154

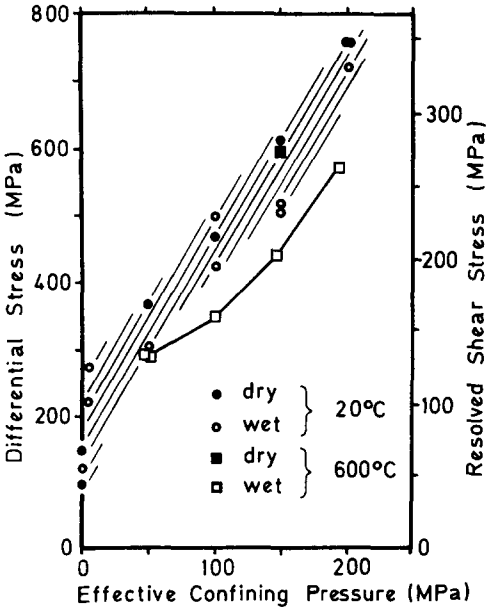

Fig. 4. Stress supported after 1.5 mm specimen shortening from curves shown in Fig. 3, plotted against effective confining pressure (total confining pressure minus pore pressure). The shading brackets all of the test results except the 600°C wet results. There is no significant difference in behaviour between the wet and dry behaviour at 20°C and the dry behaviour at 600°C. Samples deformed wet at 600°C appear to be slightly weaker at higher effective pressures. Under all conditions the behaviour of these samples is consistent with predictions based on the effective stress principle. A scale of resolved shear stress along the sawcut is also shown.

mineralogy of new phases in deformed samples by X-ray diffraction, but the small size of the samples together with the small volume fraction of new phases (~10%) made the results inconclusive.

EXPERIMENTAL RESULTS

Mechanical data

Mechanical data are given in Figs. 3–6. Data are shown corrected for the strength of the copper jacket and for axial apparatus distortion. Displacements are

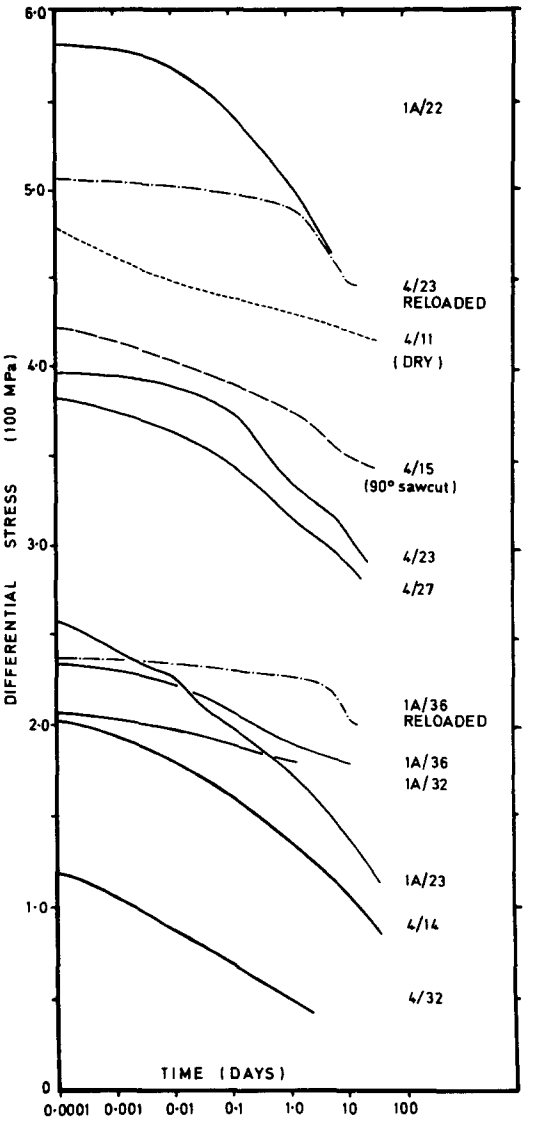

Fig. 5. Differential stress vs log time curves for stress relaxation experiments (see Table 2 for experimental details). Curves are also shown for the relaxations following reloading of samples 4/23 and 1A/36.

Table 2. Stress relaxation experiments

Test Nr.	Wet/dry	Temp. T°C	Sawcut Orient.	Conf. Press. MPa	Hollow spec.?	Pore Press. MPa	Start stress MPa	Duration days
4/21	dry	600	35	150	no	0	480	32
4/15	wet	600	90	160	no	23	425	32
1A/22	wet	600	35	160	yes	22	580	8
4/23	wet	600	35	170	no	21	396	22.4
4/23*	wet	600	35	170	no	21	506	15.8
4/27	wet	600	35	170	no	21	385	16.6
1A/32	wet	600	35	170	yes	26	206	2
1A/36	wet	600	35	170	yes	21	234	12.6
1A/36*	wet	600	35	170	yes	21	240	16.2
1A/23	wet	600	35	160	yes	107	260	32
4/14	wet	600	35	160	no	21†	203	40
4/32	wet	600	35	163	yes	108	125	2
Hydrostatic heat treatment:								
4/22	wet	600	—	200	—	200	—	42

* Reloaded.
† Thought to be about 200 MPa, accidentally impounded.

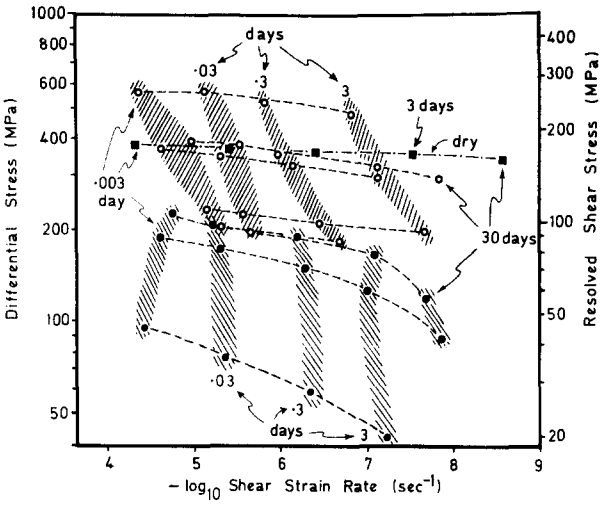

Fig. 6. Plot of differential stress and shear stress resolved along the sawcut (log scales) vs total apparent shear strain rate (axial shortening rate resolved along sawcut direction, divided by gouge thickness) for 600°C stress relaxation experiments (Fig. 5 and Table 2). Dashed lines show individual stress relaxation curves. Data points show strain rates after 0.003, 0.03, 0.3, 3.0 and 30 days elapsed relaxation time. Results from different tests but after the same elapsed time are linked by shaded areas. Open circles = low pore pressure tests; closed circles = high pore pressure tests (see Table 2). From the steepness of the shaded areas a low sensitivity of strain rate to stress is inferred, assuming comparable microstructures after a given elapsed time. In principle, extrapolation of the curves for individual tests to the right would give the rheological characteristics of a near zero porosity gouge, i.e. intact basalt.

given measured parallel to the specimen axis rather than resolved parallel to the sawcut, because the axial displacement resolves itself into imprecisely known axial and shearing components. Distortion-producing stresses are given both as differential stress (σ_1–σ_3) and shear stress resolved parallel to the sawcut orientation. Reproducibility of the force gauge calibration is such that reported differential stresses are expected to be correct within ±10 MPa. The gouge thickness may vary within about 10%, and is probably the principal source of variability of mechanical behaviour between specimens.

Figure 3 shows that the mechanical behaviour of the basalt gouge is characterized by a marked sensitivity to confining pressure, together with rapid strain hardening. The strain hardening implies that the cataclastic deformation is distributed throughout the gouge zone, which was confirmed through microstructural study. At high strains the development of distributed Riedel shears was perceptible.

From Fig. 3(a), comparing the 20 and 600°C data dry and wet (λ = 0 = pore pressure/confining pressure, at 20°C or at λ = 0.05 at 600°C), it is seen that the presence of water does not affect greatly the behaviour of the gouge. The stress/displacement curves at 20 and 600°C at different λ values are shown in Fig. 3(b). Comparing Figs. 3(a) and (b), it is apparent that at this deformation rate, at both temperatures, the strength of the gouge is reduced by pore pressure in accordance with the effective stress principle. On Fig. 4, stress levels supported at 1.5 mm axial displacement are plotted as an index of the level of the stress/displacement curve vs effective confining pressure (total confining pressure minus pore water pressure). The plot indicates the effect of wetting and the effectiveness of the pore pressure over a wide pressure range at 200 MPa total confining pressure.

There is no indication of dilatancy hardening nor of anomalous weakness, relative to strength predicted from the effective stress principle, in the elevated pore pressure tests at the strain rate used. No difference in behaviour was seen between samples with and without a fluid access hole drilled in the upper specimen half. These results indicate that the permeability of the intact basalt was sufficient to allow pore pressure equilibration in response to gouge porosity fluctuations in a time scale of the order of 10 min, following a period at temperature and in the presence of water of less than one day. Such behaviour demands a permeability at least of the order of 10^{-19} to 10^{-20} m^2. Establishment of this pattern of behaviour is necessary in order to permit interpretation of the long duration, high temperature tests.

Figure 5 shows stress relaxation results at 600°C. At any point on the stress relaxation curve the instantaneous permanent strain rate is proportional to the negative of the stress relaxation rate, the constant of proportionality being a combined machine plus specimen compliance factor. Thus a single stress relaxation curve gives some idea of the rheological behaviour of the material, the variation of strain rate over a range of stress. For our 600°C experiments a stress relaxation of 100 MPa is estimated to be equivalent to a permanent strain of 0.20 within the sheared zone. Relative shear-strain rates obtained from stress relaxation rates are thought to be correct to within a factor of two or three, whereas absolute strain rates can probably be estimated to no better than one order of magnitude. Machine relaxation (using a dummy Nimonic alloy specimen) was checked at 600°C at 1 GPa and at 500 MPa differential stress. It was found to be negligible at the higher stress and undetectable at the lower. Similarly, relaxation of intact wet (100 MPa pore pressure) basalt at 600°C and 500 MPa differential stress was negligible compared to that of the gouge filled sawcut samples.

One of the most significant problems of interpreting rheological behaviour from stress relaxation curves arises from the fact that the microstructure generally evolves with permanent strain accumulated during the relaxation (Rutter *et al.* 1978). For example, a non-linear viscous material deforming at constant microstructure over the stress range of the relaxation would exhibit behaviour characterized by

$$\mathrm{d}\log(\mathrm{d}\sigma/\mathrm{d}t)/\mathrm{d}\log t = n,$$

in which n is the exponent of the flow law, $\dot{e} \propto \sigma^n$, which would be unity for a Newtonian viscous material, and greater than, or less than one for more general non-linear behaviour. σ is the flow stress at strain $\dot{e}$ and t is elapsed time.

On the other hand, for a linear viscous material which displayed strain hardening (implying microstructural change during the relaxation) the stress relaxation test would yield an apparent value $n > 1$. n would appear larger the greater the strain hardening rate. The reverse

applies for strain softening. This problem was expected to be especially acute in this study because of the observed dramatic modification of the microstructure that occurs during hot, wet working (see later). Two specimens were reloaded after relaxation (Fig. 5). The different form of relaxation behaviour after reloading may be interpreted to mean that significant microstructural change accompanies stress relaxation.

Figure 5 shows that the stress relaxation curves collectively cover a larger range of stress than does a single one. Different relaxation tests were started after different amounts of post-yield strain, which covers a large stress range because of strain hardening. Thus each relaxation starts at a particular microstructure, though the differences between them are due to different amounts of cataclastic deformation.

The wet sheared samples should be compared to the dry one and to the wet sample with a sawcut normal to the compression direction. Compared to the latter two curves, all the wet sheared specimens show relatively rapid rates of stress relaxation after times in excess of about 3 hours. This is interpreted to mean that relaxation is facilitated by the presence of water and that the relaxation is not due simply to enhanced compaction of the gouge but involves additional shearing displacements.

The relaxation curves for the wet sheared samples are remarkably similar in form to each other. Strain rates after a given elapsed time for the different curves are very similar, the variation being far less than the strain rate variation along a given stress relaxation curve. This effect is illustrated in Fig. 6. On the assumptions that (i) the effect of different amounts of strain hardening during initial loading is not felt for very long after the start of stress relaxation, and that (ii) the rate-controlling microstructure varies in approximately the same way with time in all of the tests, the best indicator of the constant structure rheological behaviour is obtained from a plot of flow stress vs strain rate after equal amounts of permanent strain. Because of the similarity of the curves in Fig. 5 this is almost the same as plotting strain rates after equal amounts of relaxation time (Fig. 6). The wet sheared stress relaxation behaviour is therefore tentatively interpreted in terms of a material which at constant structure deforms at a strain rate which is almost independent of stress (i.e. $n \leq 1$), and for which the strain rate decreases markedly as the microstructure evolves.

It will be noted that the sheared stress relaxation data falls into two groups, (i) those experiments performed at 20 MPa pore pressure, which cover differential stresses ranging from 100 to 600 MPa, and which exhibited the same, high yield point during initial loading, and (ii) a group comprising tests PMB1A/23, PMB4/32 and PMB4/14. PMB1A/23 and PMB4/32 were performed at a higher pore pressure (100 MPa) and, in accordance with the effective stress principle, yielded at a low stress level during initial loading. They exhibited slightly enhanced strain rates during stress relaxation relative to the lowest stressed, low pore pressure sample (PMB1A/36). PMB4/14 (no axial hole in sample) was deformed at a nominal 20 MPa pore pressure but exhibited both relaxation and initial yield behaviour during loading comparable to PMB1A/23. It is therefore thought that this sample had accidentally impounded an anomalously high pore pressure due to a blockage in the pore pressure system. As will be seen, PMB4/14 was also microstructurally more comparable with PMB1A/23 than with the low pore pressure group of samples.

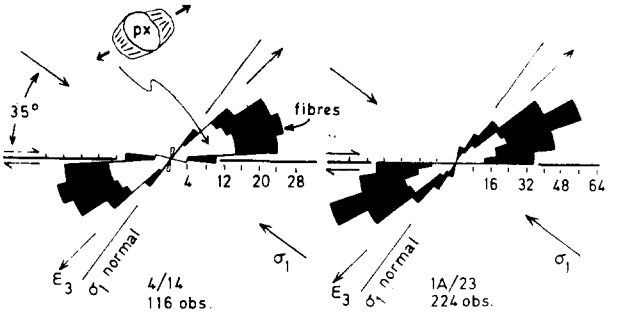

Fig. 7. Histograms showing preferred orientation of amphibole overgrowths (clear areas) and mean fibre orientations within overgrowths (black areas). Optical measurements from samples PMB1A/23 and PMB4/14. Shear zone orientations and applied compression directions are also shown. Incremental extension directions (ϵ_3) are shown assuming simple shear parallel to the sawcuts.

Microstructural observations

In all the wet high-temperature experiments run for a few days or more, mineralogical changes were observed. These involved the formation of overgrowths of amphiboles and feldspars developed on all, variously oriented, pre-existing phases in dilatant interfaces and original pore spaces. Amphiboles plus feldspars developed only in the high pore pressure runs (PMB4/14 and PMB1A/23), whereas only feldspars developed in the low pore pressure runs. The development of preferred orientation was apparent only in the case of amphibole overgrowths. However, a marked foliation was developed in low pore pressure samples which had been deformed to high strains. These structural features are described separately below.

Overgrowths exhibiting preferred orientation. Most attention is given here to the microstructure of the high pore pressure wet sheared samples. After stress relaxation for 30–40 days alteration effects could be discerned optically in the form of fibrous or platy in infillings of pore spaces and the formation of oriented mineral overgrowths several microns long (shown later to be amphiboles) on the parts of the boundaries of pre-existing grains subjected to extension (Fig. 12).

The orientations of the traces of overgrowth fibres and the patches that contain them were measured optically (Fig. 7). Measurable overgrowths were best seen on the larger pyroxene clasts surrounded by finer-grained feldspars. In both samples the preferred overgrowth orientation implies dilation in a direction lying between the sheared zone walls and the incremental extension direction (assuming simple shear). Because about half of the strain in the gouge zone is due to compaction (based

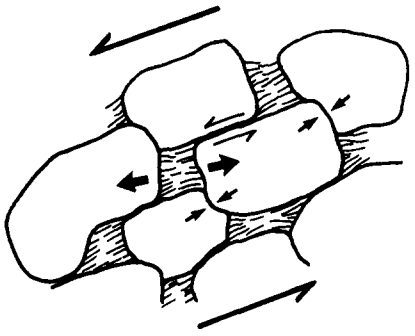

Fig. 8. Schematic illustration to show the interrelationships between dilation direction, fibre growth and grain boundary sliding in the direction of greatest resolved shear stress. Overgrowths and hence rock fabric may not therefore be simply related to finite strain principal directions during non-coaxial deformations.

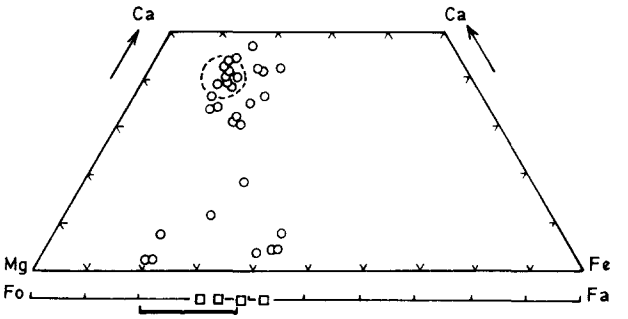

Fig. 9. TEMSCAN analyses of 30 pyroxenes (open circles) and four olivines (open squares) from samples PMB1A/23 and PMB4/14. Dashed circle and bar scale indicate coresponding ranges for samples from same locality reported by Esson *et al.* (1975).

on result of PMB4/15), the strain due to shear parallel to the gouge zone boundaries is about $\gamma = 0.1$. Thus if the preferred orientation represented dilation in the finite extension direction it would be expected to lie at about 40° to the sheared zone walls, the effects of compaction strain tending to increase this angle still further. However, the maximum dilation lies about 25° to the sheared zone walls. If interpreted as representing the finite extension direction during simple shear a figure $\sim\gamma = 2.0$ would be obtained. The discrepancy may arise because the deformation is heterogeneous on the grain scale, involving sliding between rigid mineral grains. We might suppose that the most favoured interface for sliding would be that sustaining maximum resolved shear stress. Assuming homogeneous stress and no stress refraction across the sheared zone boundary this will be at 45° to the cylinder axis, or about 10° to the shear zone walls. The formation of overgrowths by such sliding is illustrated schematically in Fig. 8. Bearing in mind the effects of compaction, which would tend to increase this value, the observed preferred orientation is fairly consistent with this suggestion, which could be investigated further by shearing gouge in sawcuts of different orientations.

The single run carried out wet at 600°C under hydrostatic stress conditions (PMB4/22) showed the development of amphibole overgrowths which, as expected, showed no preferred orientation.

The overgrowths and pore fillings could be rendered more spectacularly visible by scanning and transmission electron microscopy. Figures 13 and 14 show examples of oriented platy and fibrous minerals developed between pre-existing grains. The SEM photographs in particular show how the pre-existing porosity (about 30%) is almost completely filled. It is thought that such a gross modification of the microstructure with time will greatly modify the rheological behaviour.

Feldspar overgrowths. Although amphibole overgrowths developed only in samples tested at high pore pressure, in both these tests and those performed under low pore pressure both new and pre-existing void spaces tended to become filled with (non-fibrous) plagioclase feldspar overgrowths. These were seen in TEM to be structurally continuous with pre-existing feldspar clasts, with no discernible microstructural discontinuity at the host–overgrowth interface. Feldspar cementation was best seen in SEM using secondary or backscattered electron imaging (Figs. 14 and 15). It is discernible because of the loss of most of the initial porosity, the infilling of initial re-entrants between pyroxene clasts and the formation of trails of cuspate voids where growing crystals coalesce.

In runs like PMB1A/22, which were stress relaxed from a high differential stress at low pore pressure, localized high strain belts developed, oriented obliquely to the shear zone walls (Fig. 15). These zones developed in the R_1 Riedel shear orientation, which is the same orientation relative to shear direction as displayed by "extensional crenulation cleavage" (Platt & Vissers 1980) or "shear bands" (e.g. Gapais & White 1982). They are bands of enhanced cataclasis of feldspar, pyroxene, olivine and magnetite, developed mainly during initial, high strain rate deformation. Large original clasts are strung out into trails in the finite extension direction. During relaxation, void spaces become almost totally filled with recrystallized plagioclase.

The resulting strongly foliated microstructure is reminiscent of some naturally occurring mylonitic rocks. The cementation of feldspar-rich areas by structurally continuous overgrowths produces optically a fine-grained but porosity-free rock. Fragments in some elongate stringers often are displaced but not rotated with respect to one-another, so that elongate grains result after cementation. If taken to completion, the texture resulting from these processes could in some instances easily be confused with the products of plastic deformation accompanied by intense dynamic recrystallization.

Composition of the new phases. Energy dispersive analyses have been made by TEMSCAN of overgrowths and host phases in samples PMB4/14, PMB1A/23 and PMB4/27. Results are summarized in Figs. 9–11. From the spectra it was fairly straightforward to distinguish between the main mineral groups. The analyses obtained, however, are only regarded as being of semi-quantitative significance. The problem of sodium volatilization in the electron beam is regarded as a significant contributor to a large scatter for repeat analyses on feldspars (Fig. 10). Anorthite content in

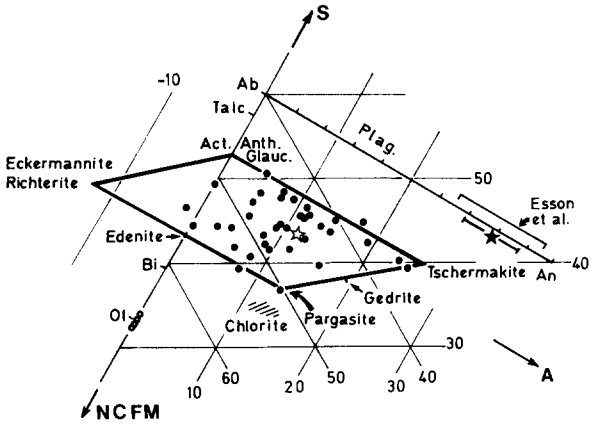

Fig. 10. Composition of 38 amphibole overgrowths from samples PMB1A/23 and PMB4/14, expressed on ternary diagram with apices S = Si^{4+}, A = Al^{3+} + Fe^{3+} + $2Ti^{4+}$ − Na^{+} − K^{+}, NCFM = Ca^{2+} + Fe^{2+} + Mg^{2+} + Mn^{2+} + $2Na^{+}$ + $2K^{+}$ − Ti^{4+} (Robinson *et al.*, 1982). The open star indicates averaged composition (Table 3) (Mg gedrite or cummingtonite). The emboldened area encloses the compositional limits of amphiboles. Other idealised mineral compositions are also shown, together with TEMSCAN analyses of host olivines (open circles) and feldspars (closed star). Error bars around the closed star indicate ± one standard deviation for the 48 feldspars analysed (composition based on Al/Si ratio). Range bar for analyses reported by Esson *et al.* (1975) also shown.

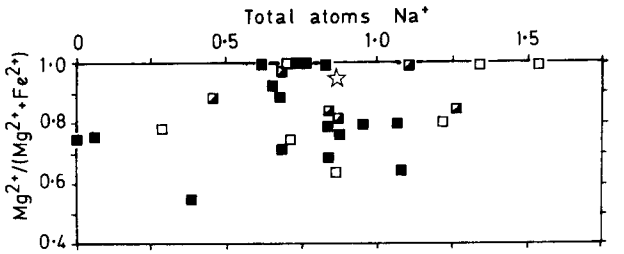

Fig. 11. Host/overgrowth composition relations in terms of Mg^{2+}/(Mg^{2+} + Fe^{2+}) and total atoms Na^{+} in amphibole overgrowths. Open symbols, feldspar hosts; closed symbols, pyroxene or olivine hosts; half closed symbols, pyroxene and feldspar hosts; star, average amphibole composition (38 analyses). There is no significant host/overgrowth composition correlation. Note relative Mg^{2+} enrichment in all amphiboles.

plagioclase would differ by up to 20% when calculated from the Al/Si ratio on one hand and the Na/Ca ratio on the other. The problem is exacerbated through the difficulty of obtaining quantitative analyses from specimens such as these which may vary widely in thickness and surface roughness and which are very fine grained. Contributions to spectra from grains surrounding the one of immediate interest may contribute significantly to scatter in the results, especially when iron rich minerals are present (Jefferson 1982). These experimental samples are also very unstable during and after thin foil preparation, when release of stored strain energy can cause the foil to disintegrate. It is unusual for a foil to survive more than one or two TEMSCAN sessions, and it is unusual to be able to obtain more than two or three successful foils from a test specimen in the first place.

Amphiboles were only formed in the higher pore pressure samples, as might be expected from their stability relations (Spear 1981). Analytical results are shown in Fig. 10, which serves to show that all of the fibrous/platy overgrowths appear to be amphibole, rather than talc, for example. Mottl & Holland (1978) found that talc was a significant alteration product of basalt in hydrothermal experiments at 500°C. All of the analyses from the fibrous/platy overgrowths were processed by the method of Papike *et al.* (1974) to differentiate Fe^{3+} from Fe^{2+}. About half of the analyses failed to meet the stoichiometry requirements of amphiboles, and this is attributed to analytical uncertainties of the types discussed above.

The compositions of the amphiboles are concentrated in the field of the most commonly occurring amphiboles in nature. Because of analytical uncertainties it is not known the extent to which the apparent spread of compositions is real. All of the amphiboles exhibited high values of Mg^{2+} relative to Fe^{2+}. This is illustrated in Fig. 11 for those amphiboles which had grown on or between identified hosts. $Mg^{2+}/(Mg^{2+} + Fe^{2+})$ is plotted against total Na^{+} to seek possible correlation between amphibole composition and host composition. No significant correlation was found. This, together with the observation that the overall spread of analyses between different grains of the same mineral is commensurate with repeat analyses on the same grain suggests that all of the amphibole overgrowths may have approximately the same composition. This may also be expected given the high porosity of the rock and the likelihood of vigorous convective circulation of water in the pore spaces. An average amphibole composition was therefore calculated from the 38 analyses obtained (Table 3), and may be described as an Mg gedrite or cummingtonite.

Table 3

Average of 37 amphibole analyses

Oxides	Si	Al	Mg	Fe	Mn	Ti	Ca	Na	K	Sum
Wt.%	49.52	8.12	12.26	22.47	0.33	0.38	3.84	2.96	0.37	100.25
Std. dev.	3.24	4.59	4.72	5.25	0.44	0.40	3.22	1.33	0.56	

Cations per 23 oxygens

Si	Al(IV)	Al(VI)	Ti	Fe^{3+}	Mg	Fe^{2+}	Mn	Ca	Na(M4)	Na(A)	K
6.70	1.23	0.00	0.04	1.27	4.53	0.12	0.04	0.56	0.45	0.33	0.64

Cation sum = 15.40

Whole rock analyses (from Esson *et al.* 1975), Sample numbers 311 and 309

Oxide	Si	Al	Fe^{3+}	Fe^{2+}	Mg	Ca	Na	K	Ti	Mn	H_2O^{+}	Sum
Wt.%												
311	46.50	15.74	2.55	8.74	9.22	12.48	1.87	0.14	1.14	0.21	1.14	100.1
309	46.35	15.76	2.43	8.83	9.12	12.81	1.84	0.14	1.13	0.21	1.89	100.5

DISCUSSION OF EXPERIMENTAL RESULTS

The results of the short duration, constant displacement rate tests serve mainly to verify that the rock obeys the principle of effective stress, and need not be discussed further here.

The long duration wet stress relaxation tests at 600°C show clearly that deformation experiments can be carried out on a basaltic rock accompanied by substantial amounts of chemical transformation. Comparison of stress relaxation curves obtained from wet samples having a 35° sawcut, with those from wet samples having a 90° sawcut orientation, show that (a) deformability is enhanced by the presence of water and (b) deformation is due not only to compaction and pore elimination, but involves shearing parallel to the sawcut, each process contributing to the strain by about the same amount.

As sample PMB4/22 shows (600°C, wet, hydrostatic stress), the amphibolitization of a basalt occurs spontaneously. The only feature suggestive of any relationship between deformation of these samples and the chemical change is the development of amphibole overgrowths with a consistent preferred orientation. Overgrowths clearly develop preferentially on less stressed, potentially dilatant interfaces, and are only rarely seen in interfaces sustaining high resolved shear and normal stresses. Feldspar overgrowths may well develop in this way, but it is not obvious if they do because there is no chemical, optical or otherwise discernible contrast with respect to host grains.

Deformation mechanisms

As mentioned earlier, the amphiboles are best developed growing in directions of greatest resolved shear stress, and for this reason it is suggested that deformation during stress relaxation involves a significant component of diffusion-accommodated grain-boundary sliding (incongruent pressure solution), the diffused components of feldspar, pyroxene and olivine in the intergranular aqueous phase then reacting to produce amphibole and feldspar in the dilatant, relatively unstressed interfaces. This interpretation is supported by the inference from the stress relaxation results that the strain rate is very insensitive to stress after a given degree of microstructural evolution, an expected characteristic of diffusive mass-transfer processes (Rutter 1976, 1983).

The latter inference is subject to the correctness of the interpretation of the single stress relaxation curves in terms of hardening associated with the microstructural change which accompanies strain. For each curve the hardening corresponds to between two and three orders of magnitude in strain rate for a shear strain of about 0.2. A very effective hardening process can be found in the tendency for contact areas to increase as overgrowth development proceeds. For creep controlled by grain boundary diffusion the strain rate varies inversely as the cube of the grain contact diameter. Thus an increase of average grain contact diameter of $\times 10$ would reduce the creep rate by $\times 1000$. This is consistent with the observed microstructural evolution and the decay of strain rate with time.

It is inevitable that during the early stages of stress relaxation some of the deformation is by cataclasis. Because this is a pressure-sensitive process, with further experiments at different effective confining pressures it will be possible to evaluate its relative importance at various stages of stress relaxation. Cataclastic flow may be time dependent through the processes of subcritical crack growth (Atkinson 1982), but stress is not expected to be strongly strain-rate sensitive when this process is dominant.

Creep by diffusive mass transfer processes, especially when there is a molar volume change (ΔV) between consumed and precipitated phases, necessarily involves grain boundary sliding displacements (Raj & Ashby 1971). Only when $\Delta V = 0$, when porosity is zero, and the rate of infilling of potentially dilatant volume exactly matches the rate of dilation will the flow be at constant volume and hence pressure insensitive. There can be a complete spectrum of variation between flow purely by pressure-insensitive diffusion mass transfer plus grain-boundary sliding, and fully pressure-sensitive cataclastic flow. It is thought that the flow in our experiments lies some way between these extremes. Such mixed mechanism flow was proposed to explain the creep of mixed clay/quartz fault gouge in experiments by Rutter & Mainprice (1978).

Intracrystalline plastic deformation is not thought to be significant in these experiments. No evidence of significant dislocation activity was seen in HVTEM study. Further, Caristan (1982) found that temperatures in excess of 800°C were necessary at moderate confining pressures for pressure insensitive plastic flow in basalt.

Effect of the chemical changes on resistance to deformation

Because of the large initial porosity of the test material, it is not expected that the increase in volume of the solid phases which accompanies hydration (assuming no loss of material in the convective circulation of the pore fluid) will induce stresses which will assist intracrystalline plastic deformation. However, we may examine the effect of the reactions on the stress-induced chemical potential gradients driving intergranular diffusion.

The formation of Mg gedrite from starting materials dominated by plagioclase, augite and olivine requires reaction between either olivine and plagioclase, augite and plagioclase, or both

$$\text{pyx} + \text{plag} + H_2O = \text{Mg gedrite} + Ca^{2+} + Si^{4+}$$
$$\text{ol} + \text{plag} + H_2O = \text{Mg gedrite} + Ca^{2+} + Si^{4+}$$

(numbers of molecules are not implied). New mineral growths rich in calcium were not found in the samples, and it is thought that calcium and silica were removed by hydrothermal convection and precipitated in the cooler parts of the pore pressure system.

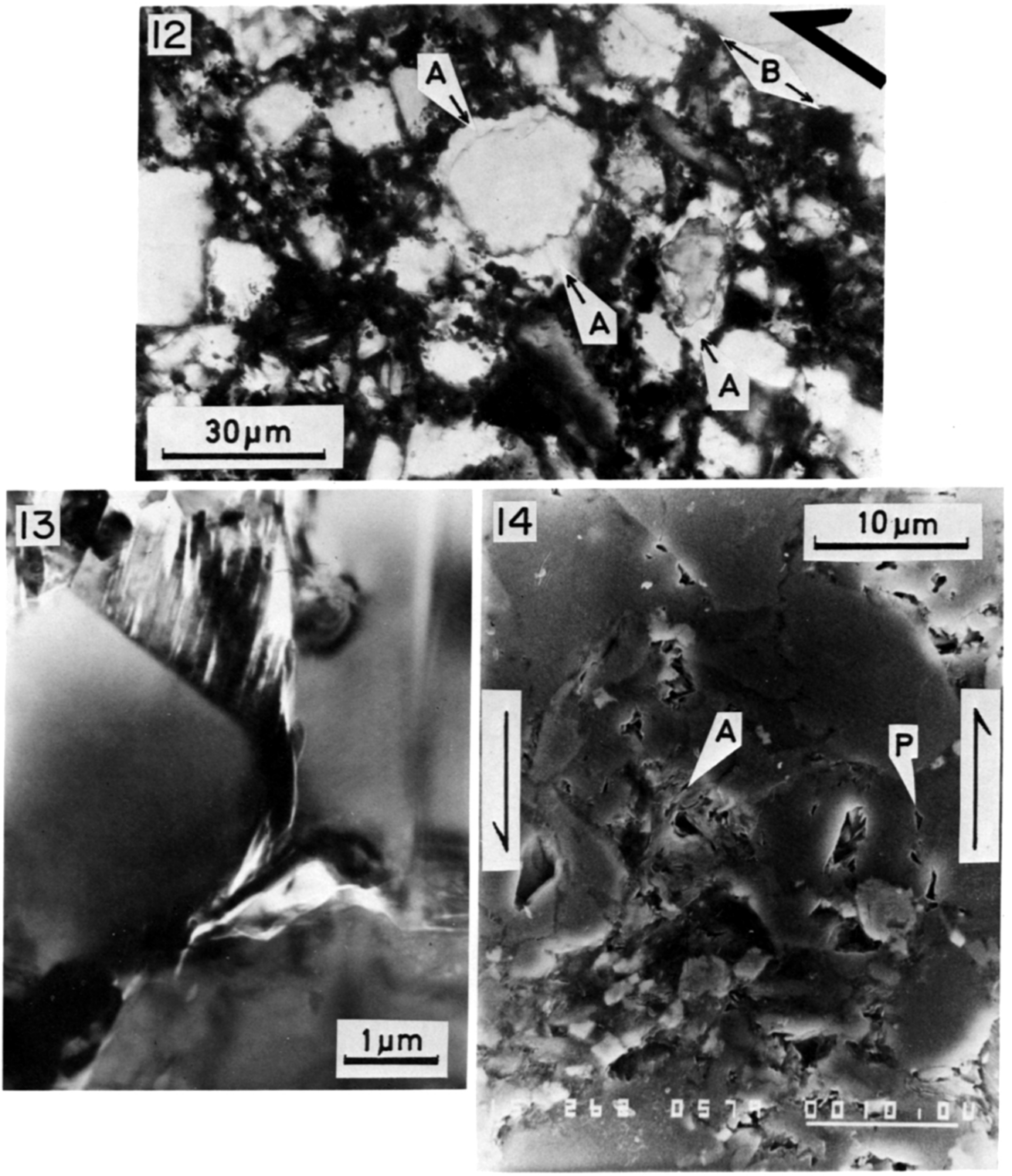

Fig. 12. Optical micrograph showing typical oriented, fibrous amphibole overgrowth (indicated A) developed on a large pyroxene grain. The edge of the sheared zone can also be seen (B) (specimen PMB4/14).

Fig. 13. High voltage TEM micrograph showing oriented amphibole overgrowth developed on host pyroxene grain (specimen PMB4/14).

Fig. 14. Secondary electron image of polished surface of a specimen (PMB1A/23) deformed at 600°C at high pore pressure, showing (i) development of oriented amphibole (A) overgrowths and (ii) filling of porosity by feldspar overgrowths, often leaving trails of voids (P) along impingement interfaces. The shearing direction is indicated.

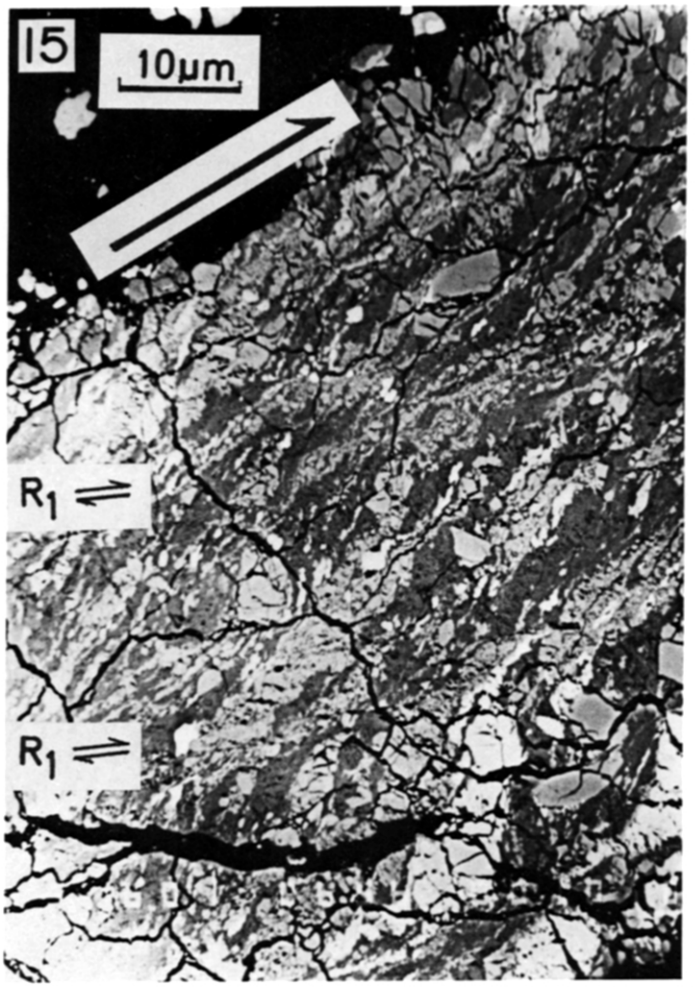

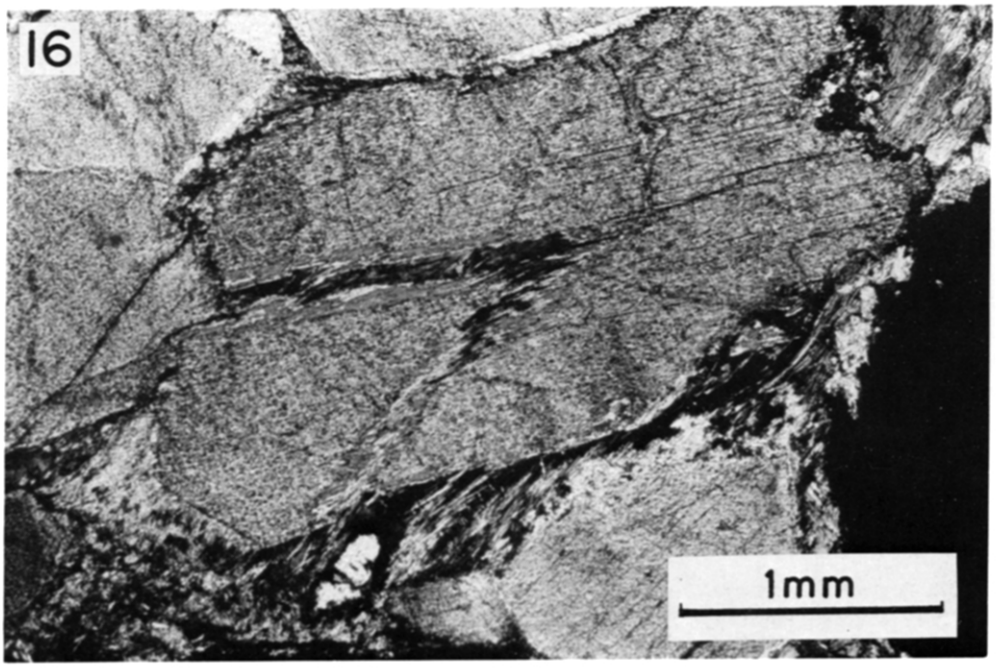

Fig. 15. Backscattered electron image (atomic number contrast) of specimen PMB4/21, deformed at 600°C at low pore pressure. Crushed grains of pyroxene and plagioclase are strung out at about 30° to the shearing direction and are almost completely cemented by overgrowths of plagioclase (dark grey relative to light grey of pyroxene). Incipient formation of shear bands in the R_1 Riedel shear orientation (indicated) can be seen. The black sinuous traces are cracks in the specimen surface introduced during specimen preparation.

Fig. 16. Optical thin section of naturally deformed Lewisian hornblendite (Lochalsh, Scotland), showing cracking of grains and growth of oriented fibrous actinolite and chlorite filling dilatant voids between grains and fragments.

In order that creep can be achieved by stress-induced diffusive mass transfer in an intergranular aqueous film, the water in the interface must be able to sustain a pressure gradient without flowing. It must therefore be structured through adsorption onto the mineral surfaces and, for mechanical equilibrium, must everywhere sustain the same interfacial stress as the solids. The swelling of mineral interfaces against a substantial applied stress, due to water adsorption, can be demonstrated experimentally (e.g. Rutter 1983). This osmotic pressure profile will be associated with a lower water activity profile arising from the stress induced gradient of chemical potential of the 'dissolved' components of the solid phases. Even in the pore spaces the water activity will be lowered by the dissolved solids.

The general principles of the derivation of the flow law for creep controlled by water assisted diffusive mass transfer are reviewed by Rutter (1983). For such creep the flux of matter is driven by the gradients of chemical potential, μ_n, of the n components of the solid phases in the intergranular aqueous films. Even if the overall strain rate is controlled by growth kinetics at points of precipitation of diffused material, because diffusion creep involves a sequence of processes, of which diffusion is one, it is in principle always possible to describe the flow rate of the aggregate in terms of the stress induced diffusion of a single chemical component.

For steady state creep the geometry of the stressed interface must remain constant for a reasonable increment of strain, and a particular profile of μ along the interface must become established in order to satisfy Laplace's equation, $\nabla^2\mu = 0$. The exact profile depends on the interface shape. For example, in the case of a flat, circular interface of radius a (Rutter 1976), it is parabolic. This is shown in Fig. 17(b) (dashed curve). The variation of μ with radial distance r along the interface can be made parabolic by varying the stress distribution (Fig. 17b) subject to the condition of mechanical equilibrium, which in this case is given by

$$\pi a^2 \sigma_1 = 2\pi \int_0^a r\sigma(r)\, dr$$

for the σ_1 direction. This equilibrium will be established early in the creep by diffusive redistribution of material.

Appealing to a reduced activity of water in the central, more highly stressed regions of grain/grain interfaces (whilst the effective water pressure equals the interfacial stress as required for mechanical equilibrium) means that the solid phases adjacent to the more stressed parts of the interfaces will remain anhydrous. In contrast, the outer regions and the pore spaces will hydrate, provided the pore-water pressure is sufficiently high. Lower differential stress will cause hydration to affect more completely all grain interfaces. All extremes of this behaviour are seen in our experimental results. At low P_{H_2O} (20 MPa) at 600°C, σ_3 = 150 MPa and $(\sigma_1-\sigma_3) >$ 200 MPa, amphibole is either not stable or its appearance is inhibited by kinetic factors (cf. Spear 1981), thus only feldspar overgrowths are seen. At $P_{H_2O} = P_{total}$ and $(\sigma_1-\sigma_3) = 0$ (PMB4/22), hydration occurs at all interface orientations and an isotropic texture results. At P_{H_2O} = 100 MPa, σ_3 = 150 MPa and $(\sigma_1-\sigma_3)$ = 150 MPa amphibole formation is suppressed over relatively stressed interfacial orientations. The textural observations made are thus consistent with this qualitative theoretical approach.

Following Paterson (1973) the most important factor determining the gradient of chemical potential driving interfacial diffusion is the product of the interfacial normal stress gradient with the molar volume of the pure solid, V_n, adjacent to the interface. Thus qualitatively, diffusive transfer may be faster along those parts of an interface which have hydrated than those parts which remain anhydrous, because of the increase in solid molar volume which accompanies hydration. Figure 17(a) shows schematically how this may increase the effective potential gradient and, through this, the creep rate, relative to diffusion creep which is not accompanied by chemical reaction. The total potential difference across the interface is increased from μ_A to μ_B. Figure 17(b) shows how the parabolic form of the interfacial normal stress must be modified when a reaction can occur along the diffusion path.

The creep rate enhancement is expected to be rather small, however, rarely as much as a factor of two or three, and will be greatest for reactions with large ΔV_{solids}. For hydration reactions like those which have occurred in the present experiments the increase in the molar volume of the solids is of the order of 10%. Therefore we conclude that in our experiments, although the metamorphic reaction is an essential part of the deformation and is expressed in the microstructure which develops, it results in no significant enhancement of creep rate. The lack of a striking enhancement of deformability during hydration is also reflected in the stress relaxation data at comparable differential stress levels for low and high pore pressure tests (PMB1A/36 and PMB1A/23, respectively). After similar relaxation times the high pore-pressure sample deforms only about ×3 faster. However, this difference may be due largely to the contrast in effective confining pressure between the two tests, so direct comparison may not be valid. In these experiments the hydration reactions also do not go to completion. If they did the rock would, of course, have different mechanical properties under given conditions because of the dominance of the new mineralogy, and would probably be softer.

The broader implications of this approach to the role of metamorphic reactions in deformation, including the rather different behaviour to be expected during syntectonic dehydration, are discussed by Brodie & Rutter (in press).

GEOLOGICAL DISCUSSION

Deformation mechanisms and microstructures

Natural deformation accompanied by hydration reactions in rocks of basic composition is very common. The

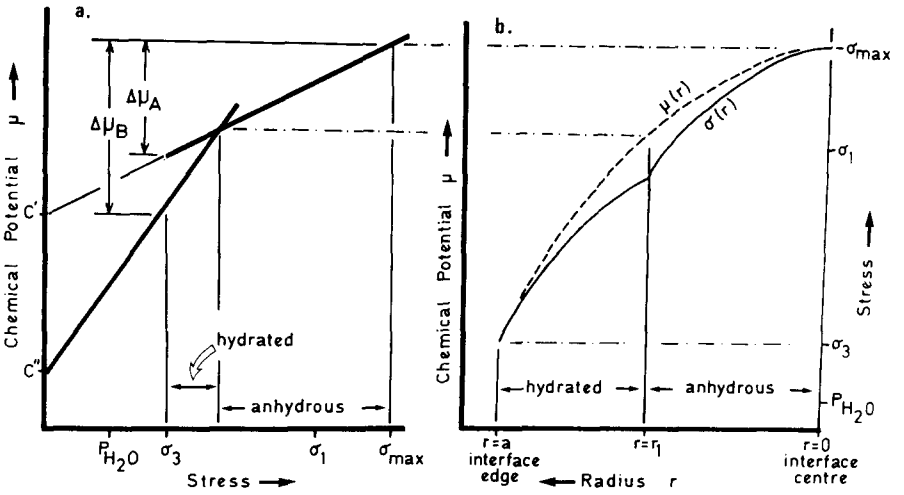

Fig. 17. (a) Schematic illustration of variation of chemical potential with interfacial normal stress, of components taking part in a balanced hydration reaction. At the intersection of the lines both of the solids and the aqueous phase are in equilibrium. Interfacial stress varies from σ_{max} ($>\sigma_1$) in the interface centre to σ_3 at the margin with a pore pressure = $P_{H_2O} < \sigma_3$. Under these conditions the solid phases in the outer part of the interface are hydrated but are anhydrous in the central part. The chemical potential difference, $\Delta\mu$, driving interfacial diffusion down the stress gradient is $\Delta\mu_A$ in the absence of reaction, but $\Delta\mu_B$ with the hydrated margin. $\Delta\mu$ is greatest of all under conditions when all of the interface is hydrated (e.g. at lower temperature for the same stress state). (b) Schematic representation of variation of interfacial normal stress, $\sigma(r)$, with r from centre to edge of the interface. The variation of μ with r is also shown (dashed), such that $\mu(r)$ satisfies $\nabla^2\mu = 0$, which is required for steady state diffusive mass transfer. $\sigma(r)$ must adjust itself and the hydration boundary shift so that the required $\mu(r)$ profile is attained. The area under the $\sigma(r)$ curve must also equal the product of σ_1 with the interfacial cross sectional area, for mechanical equilibrium.

syntectonic retrogression of initially anhydrous pyroxene granulite derived from the high grade metamorphism of basic dykes in the Lewisian complex of NW Scotland is one oft-cited example (e.g. Beach 1980). The probable interaction between metamorphism and deformation of rocks of the oceanic crust near active plate margins provides another (e.g. Girardeau & Mevel 1982).

In our long duration experiments it is inferred that deformation rate is governed by some interplay between sliding between grains, diffusive transfer of material through an interstitial aqueous phase, and growth of new phases. There was no evidence of significant intracrystalline plasticity. The type of microstructure development we observe experimentally probably gives way with increasing temperature and/or decreasing strain rate to deformation dominated by plastic deformation and dynamic recrystallization in both feldspar and mafic phases. Caristan (1982) has demonstrated experimentally a cataclastic to plastic transition in basalt experimentally deformed above *c.* 800°C when the confining pressure is sufficiently high. LaTour & Kerrich (1982), in a study of highly strained basic rocks from the Canadian Grenville province, showed that at lower temperatures (540°C by oxygen isotope geothermometry) deformation led to the development of a fibrous overgrowth microstructure, without plasticity and dynamic recrystallization, whereas higher temperature deformation (600°C) was dominated by the latter processes. Brodie (1981) has also demonstrated the role of intracrystalline plasticity and dynamic recrystallization in amphibolites deformed in shear zones under conditions corresponding to the incoming of pyroxene. Similar inferences can be made about deformation mechanisms in the retrogressive shear zones of the Lewisian complex referred to earlier (Beach 1980).

As a first-order generalization, therefore, we might expect that high temperature (>600°C) natural deformation of basic rocks is dominated by intracrystalline plastic processes, passing into flow by diffusive transfer plus grain sliding and fracturing processes at lower temperatures. A good natural example of the latter process is provided by the deformation of a hornblendite dyke in the Lewisian rocks which are involved in the Moine thrust belt in the Lochalsh district of Scotland, 300 m east of the summit of Carn a'Bhealaich Mhoir (GR 831323). The microstructure of this rock is illustrated in Fig. 16. Crystals of hornblende are broken by transgranular cracks and the fragments are displaced and rotated slightly. An oriented fibrous overgrowth of actinolite plus chlorite is developed in the dilatant regions between hornblende grains. Stylolite surfaces truncate and cross many grains and have a preferred orientation which contains the overgrowth dilation direction (Fig. 18).

This rock provides a natural analogue of our experimental runs where oriented amphibole overgrowths were produced. In the natural example the retrogressed, more hydrous mineral assemblage is preferentially developed in interfaces sustaining relatively low interfacial normal stress, and the diffusion creep is developed in a rock which had suffered cataclastic deformation earlier in the progression of the deformation. The dilation accompanying this cataclasis may have been instrumental in allowing access to sufficient water for the retrogression reactions. As with the experimental samples, although the microstructural arrangement of the new mineral phases is in direct response to the deviatoric

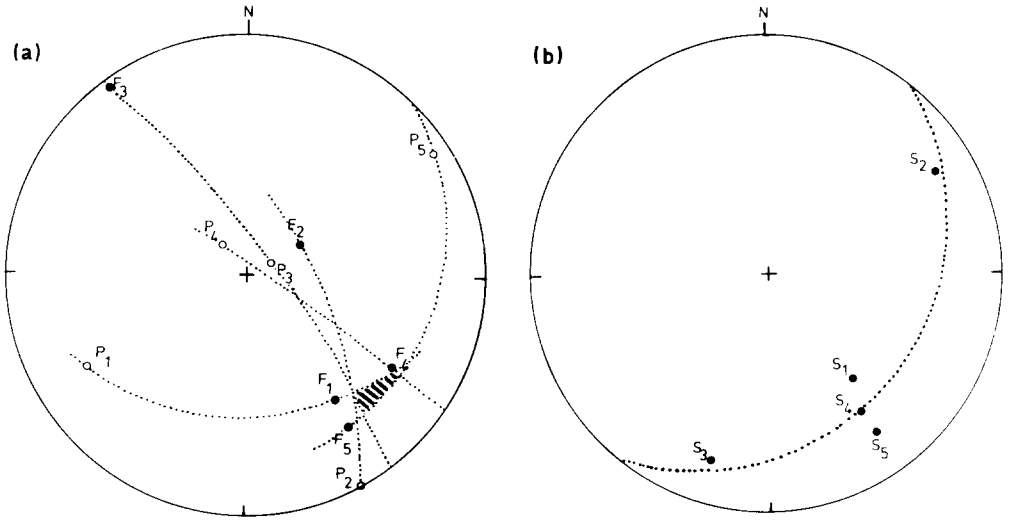

Fig. 18. Preferred orientation of fibrous amphibole overgrowths (a) and stylolites (b) in partially retrogressed hornblendite from Lochalsh, Scotland (see Fig. 16). Measurements were made of linear traces on five differently oriented thin sections of between 90 and 120 fibre orientation per section and 10 stylolite orientations per section. Standard deviations for stylolite orientations ranged between 7 and 14°, and for fibre orientations between 24 and 31°. Dashed curve in (b) shows estimate of stylolite 'foliation' orientation (great circle containing five traces S_{1-5}). Great circles in (a) join poles to thin section orientations (P_{1-5}) to corresponding traces of mean fibre orientation (F_{1-5}). Their intersection estimates fibre orientation in space. Shaded area shows most likely fibre orientation, which lies down dip on the stylolite plane.

stress environment, the syntectonic reactions probably do not lead to substantial softening of the rock, but do provide evidence that the presence of a moderate water pressure was essential to the deformability of the rock.

In this particular natural example the role of cracking and grain displacements is evident optically because, as a result of deformation at a lower metamorphic grade, mineral growths which fill the voids are mineralogically and texturally distinct from the host grains. In our low P_{H_2O} experimental samples feldspar overgrowths cannot be distinguished from their host crystals, except where they are pyroxenes or olivines, either on the basis of composition, structural orientation or internal microstructure in the final rock product of the experiment. It is only by comparison with the known starting material that cementation can be demonstrated. Thus in natural deformation under conditions where product phases will be mineralogically similar (though they may exhibit solid solution compositional variations) to starting phases, it is possible that a rock which had suffered grain size reduction by cataclasis plus cementation by diffused material would be optically indistinguishable from one which had suffered grain size reduction by dynamic recrystallization. The role of cataclasis plus cementation in natural, highly strained basic rocks, and rocks of other compositions, remains to be more fully evaluated (but see Brodie & Rutter in press). Studies of the past decade may have created an out of balance view of the relative importance of intracrystalline plastic versus dilatancy producing (cataclastic) processes in the development of many mylonitic rocks. For example, recent microstructural studies of quartzo-feldspathic mylonites (White *et al.* 1982, White & White 1983, White in press) have outlined the variable roles of cataclasis and retrogression on mylonitization. In some instances the low strain deformation at greenschist facies conditions is dominated by cataclasis which, because of the creation of a microstructure dominated by mechanically softer products of retrogressive metamorphic changes, gives way to plastic flow at progressively higher strains. No microstructural evidence for the earlier cataclasis remains at high strains. It is only detectable because of heterogeneity of deformation.

The significance of post-tectonic, surface energy driven grain coarsening and grain-boundary adjustments in the microstructural evolution of deformed basic rocks is a further important texture modifying factor. Relatively little data exists of the kinetics of grain coarsening in single phase rocks, and even less where two or more crystalline phases are involved. The interpretation of natural microstructures will require a better understanding of the extent to which post-deformation grain boundary adjustments can modify or destroy textures developed during deformation.

Acknowledgements—This paper was presented at the conference on 'Planar and Linear Fabrics in Rocks', held in Zurich in August 1982. Despite the forebearance of the editors, the article was not prepared in time to be considered for inclusion in the conference proceedings. This work was financed through grant aid from the U.K. Natural Environment Research Council (Grants GR/3548 and GR3/3848). Rock deformation equipment was designed and built in collaboration with N. D. Shaw and R. F. Holloway. P. Grant and P. Suddaby kindly provided their time and help with scanning electron microscopy. R. Curtis carried out X-ray diffraction analyses. R. N. Thompson suggested the Preshal Mhor locality as a suitable source for experimental material and G. Potts (Birmingham University) drew our attention to the Lochalsh hornblendite locality. K. H. Brodie provided a great deal of discussion and advice, particularly in connection with amphibole mineralogy. Two reviewers provided criticism and helpful suggestions.

REFERENCES

Atkinson, B. K. 1982. Subcritical crack propagation in rocks; theory, experimental results and applications. *J. Struct. Geol.*. **4**, 41–56.

Beach, A. 1980. Retrogressive metamorphic processes in shear zones with special reference to the Lewisian complex. *J. Struct. Geol.* **2**, 257–263.

Beach, A. 1982. Deformation mechanisms in some cover thrust sheets from the external French Alps. *J. Struct. Geol.* **4**, 137–149.

Brodie, K. H. & Rutter, E. H. in press. On the relationships between rock deformation and metamorphism, with special reference to the behaviour of basic rocks. In: *Advances in Physical Geochemistry, Vol. 4. Metamorphic Reactions: Kinetics, Textures and Deformation* (edited by Thompson, A. B. & Rubie, D. C.). Springer, Berlin.

Brodie, K. H. 1981. Variation in amphibole and plagioclase compositions with deformation. *Tectonophysics* **78**, 385–402.

Caristan, Y. 1982. The transition from high temperature creep to fracture in Maryland diabase. *J. geophys. Res.* **87**, 6781–6790.

Chaklader, A.C. D. 1975. Transformation plasticity and hot pressing. In: *Deformation in Ceramic Materials* (edited by Bradt, R. C. & Tessler, R. E.). Plenum Press, New York, 425–442.

Esson, J., Dunham, A. C. & Thompson, R. N. 1975. Low alkali, high calcium olivine tholeiite lavas from the Isle of Skye, Scotland. *J. Petrology* **16**, 448–497.

Fyfe, W. S. 1976. Chemical aspects of rock deformation. *Phil. Trans. R. Soc.* **A283**, 221–228.

Gapais, D. & White, S. H. 1982. Ductile shear bands in naturally deformed quartzite. *Textures Microstructures* **5**, 1–17.

Girardeau, J. & Mevel, C. 1982. Amphibolitized sheared gabbros from ophiolites as indicators of the evolution of the oceanic crust: Bay of Islands, Newfoundland. *Earth Planet. Sci. Lett.* **61**, 151–165.

Gordon, R. B. 1971. Observation of crystal plasticity under high pressure with applications to the Earth's mantle. *J. geophys. Res.* **76**, 1248–1254.

Greenwood, G. W. & Johnston, R. H. 1965. The deformation of metals under small stresses during phase transformations. *Proc. R. Soc.* **A283**, 403–422.

Heard, H. C. & Ruby, W. W. 1966. Tectonic implications of gypsum dehydration. *Bull. geol. Soc. Am.* **77**, 741–760.

Hobbs, B. E. 1981. The influence of metamorphic environment upon the deformation of minerals. *Tectonophysics* **78**, 335–383.

Jefferson, D. A. 1982. X-ray emission analysis in the electron microscope. *Phil. Trans. R. Soc.* **A305**, 535–543.

Kirby, S. H. 1984. Introduction and digest to the special issue on the chemical effects of water on the deformation and strengths of rocks. *J. geophys. Res.* **89**, 3991–3995.

LaTour, T. E. & Kerrich, R. 1982. Microstructures, mineral chemistry and oxygen isotopes of two adjacent mylonite zones; a comparative study. In: *Issues in Rock Mechanics, Proc. 23rd U.S. Symposium on Rock Mechanics* (edited by Heuze, F. E. & Goodman, R. E.), 389–397.

Mottl, M. J. & Holland, H. D. 1978. Chemical exchange during hydrothermal alteration of basalt by seawater—1. Experimental results for major and minor components of seawater. *Geochim. cosmochim. Acta* **42**, 1103–1115.

Murrell, S. A. F. & Ismail, I. A. H. 1976. The effect of decomposition of hydrous minerals on the mechanical properties of rocks. *Tectonophysics* **31**, 207–258.

Papike, J. J., Cameron, K. L. & Baldwin, K. 1974. Amphiboles and pyroxenes: characterisation of other than quadrilateral components, estimates of ferric iron from microprobe data. *Geol. Soc. Am. Abstr. Prog.* **6**, 1053–1054.

Paterson, M. S. 1973. Non-hydrostatic thermodynamics and its geologic applications. *Rev. Geophys. Space Phys.* **11**, 355–389.

Platt, J. P. & Vissers, R. L. M. 1980. Extensional structures in anisotropic rocks. *J. Struct. Geol.* **2**, 397–410.

Poirier, J. P. 1982. On transformational plasticity. *J. geophys. Res.* **87**, 6791–6797.

Raleigh, C. B. & Paterson, M. S. 1965. Experimental deformation of serpentine and its tectonic implications. *J. geophys. Res.* **70**, 3965–3985.

Ramsay, J. G. & Wood, D. S. 1973. The geometric effects of volume change during deformation processes. *Tectonophysics* **13**, 263–277.

Raj, R. & Ashby, M. F. 1971. On grain boundary sliding and diffusion creep. *Met. Trans.* **2**, 1113–1127.

Robinson, P., Spear, F. S., Schumacher, J. C., Laird, J., Klein, C., Evans, B. W. & Doolan, B. L. 1982. Phase relations of metamorphic amphiboles. In: *Reviews of Mineralogy, 9B* (edited by Veblen, D. R. and Ribbe, P. H.), 1–227.

Rubie, D. C. 1983. Reaction enhanced ductility: the role of solid–solid univariant reactions in deformation of the crust and mantle. *Tectonophysics* **96**, 331–352.

Rutter, E. H. 1976. The kinetics of rock deformation by pressure solution. *Phil. Trans. R. Soc.* **A283**, 203–219.

Rutter, E. H. 1983. Pressure solution in nature, theory and experiment. *J. geol. Soc. Lond.* **140**, 725–740.

Rutter, E. H. & Mainprice, D. H. 1978. The effect of water on the stress relaxation of faulted and unfaulted sandstone. *Pure appl. Geophys.* **116**, 634–654.

Rutter, E. H., Atkinson, B. K. & Mainprice, D. H. 1978. On the use of the stress relaxation testing method in studies of the mechanical behaviour of geological materials. *Geophys. J. R. astr. Soc.* **55**, 155–170.

Sammis, C. G. & Dein, J. L. 1974. On the possibility of transformational superplasticity in the Earth's mantle. *J. geophys. Res.* **79**, 2961–2965.

Spear, F. S. 1981. An experimental study of hornblende stability and compositional variability in amphibole. *Am. J. Sci.* **281**, 697–734.

Spry, A. 1969. *Metamorphic Textures.* Pergamon Press, Oxford.

Vernon, R. H. 1976. *Metamorphic Processes.* George Allen and Unwin, London.

White, J. C. & White, S. H. 1983. Semi-brittle deformation in the Alpine Fault Zone, New Zealand. *J. Struct. Geol.* **5**, 579–589.

White, S. H. in press. Brittle deformation in ductile faults and shear zones. *Proc. I.G.C., Moscow.*

White, S. H., Evans, D. & Zhong, D. L. 1982. Mylonites in the Moine Thrust Zone; microstructures and textures. *Textures Micro structures* **5**, 33–61.

White, S. H. & Knipe, R. J. 1978. Transformation and reaction enhanced ductility in rocks. *J. geol. Soc. Lond.* **135**, 513–516.